Numerical and experimental investigation of natural convection from horizontal heated cylinders

Stig Grafsrønningen

Thesis submitted for the degree of Ph.D.

Department of Mathematics
University of Oslo

December 19, 2012

Series of dissertations submitted to the
Faculty of Mathematics and Natural Sciences, University of Oslo
No. 1289

ISSN 1501-7710

Cover: Inger Sandved Anfinsen.
Printed in Norway: AIT Oslo AS.

Produced in co-operation with Akademika publishing.
The thesis is produced by Akademika publishing merely in connection with the thesis defence. Kindly direct all inquiries regarding the thesis to the copyright holder or the unit which grants the doctorate.

Preface

This thesis is submitted in partial fulfillment of the degree of *"philosophiae doctor"* (Ph.D.), at the University of Oslo, initiated in June 2009. Most of the work presented in the thesis was carried out at the Department of Mathematics at the University of Oslo, in collaboration with my main supervisor Professor Atle Jensen. Parts of the numerical and turbulence related work was conducted at the Norwegian Defence Research Establishment (FFI). Further, a small part of the work presented herein was carried out at Cornell University, Ithaca, USA, where I had a five week stay during Professor Jensen's sabbatical year.

This thesis is a collection of articles with an introduction which motivates the present work and relates the articles to each other. The main body of this thesis consist of six journal papers, which at the time of writing, four are published and the latter two are submitted and are under consideration for publication in different journals. The first five papers are published or submitted to *International Journal of Heat and Mass Transfer*. The latter paper is submitted to *Engineering and Computational Mechanics*. I am the first author of all six papers, with my main supervisor Professor Atle Jensen as co-author on all six. My co-supervisor Professor II Bjørn Anders Pettersson Reif (FFI) is co-author on two of the papers.

I have written all parts of all papers, made all plots, conducted every experiment, calibration, and post-processing of experimental data. I have further carried out all pre-processing, meshing, setup and post-processing of all simulations. The co-authors of the respective papers have contributed with ideas, extensive discussions, guidance, valuable feedback, and correction of the manuscripts.

Oslo, December 19, 2012
Stig Grafsrønningen

Acknowledgments

First I would like to express my sincere appreciation to my main supervisor Professor Atle Jensen for his excellent supervision, ideas, invaluable help and support. His solid guidance and genuine interest for my project have navigated me safely through my thesis. I would also like to thank Professor Jensen for inviting me to visit Cornell University, Ithaca, New York, during his sabbatical there. Secondly, I would like to thank my co-supervisor Professor II Bjørn Anders Pettersson Reif and the Norwegian Defence Research Establishment (FFI) for guidance and help with the turbulent simulations and other turbulence related issues throughout my project. I strongly appreciate their help and support.

Further, I am grateful to former lab-engineer at the Hydrodynamics laboratory at the University of Oslo, Svein Vesterby, for his invaluable help, before and after his official retirement. My gratitude goes also to FMC Technologies who together with the University of Oslo (UiO), and the Norwegian Research Council made it possible for me to complete this work. Financial support for this work was provided by the PETROMAKS project under research Grant No. 192215/S60 from the Norwegian Research Council (NFR).

I would like to express my appreciation to all my colleagues, co-workers and fellow doctoral students at the Mechanics Division, Department of Mathematics, University of Oslo. I really appreciate the numerous huddles, coffee-brakes, lunches and more we have had. Many ideas for my thesis have emerged from our fruitful discussions.

I would also like to thank my friends for their support and constant cheering. Finally, I would also acknowledge my family for their loving care and support. They have never stopped believing in me, and they have helped me keeping my spirit up when the going got tough, and the tough required some help to get going again.

Last but certainly not least, I would like to thank my best friend and girlfriend, Monica, for just being awesome. Your encouragement and unwavering support has been second to none. I really appreciate everything you have done for me during this project, not to mention for being my best friend whenever that was called for. I cannot fully express how your support and perpetual enthusiasm have helped me through my years as a doctoral student.

Contents

Introduction

Subsea processing is slowly maturing as an enhanced oil or gas recovery measure to increase production from marginal or mature offshore oil or gas fields. Subsea gas boosting may contribute to a substantial increased field recovery rate thus rendering economically unattractive fields attractive, or prolonging the lifetime of existing fields. Subsea heat exchangers are vital parts of subsea gas boosting modules and other subsea processing modules. Subsea gas boosting modules use large compressors to increase the gas pressure thus increasing the production rate for subsea fields. Pre- and intermediate cooling for the compressor-trains are required in order to achieve a high compressor efficiency. Subsea heat exchangers may also be used for water wellhead knockout where the produced natural gas is cooled, and water from the production stream condenses out as free water. The free water may then be separated from the natural gas and gas condensate, and is then re-injected into the reservoir without the need for further processing or without having to transport it to the topside facilities or onshore. Another use for subsea heat exchangers is cooling of the production fluid downstream the wellhead. In some cases the wellhead temperature exceeds the temperature rating of equipment further downstream, and require cooling before it is transported towards subsea processing facilities, onshore or topsides.

Various concepts for subsea heat exchangers exist, including topside-proven technology reengineered to meet subsea requirements. Passive heat exchangers are based solely on natural convection heat transfer and may have a rather simple geometry, see Figure 1 for an example. Subsea heat exchangers based solely upon natural convection heat transfer is placed in direct contact with seawater, thus an infinite cooling medium is available. Large development programs have been initiated by leading providers of technology solutions for the energy industry, see e.g. Gyles et al. [1]. Large scale experiments have been carried out by the industry, though they left some questions unanswered and raised some new questions, particularly about small scale features. This project aimed to investigate some of the small scale phenomena associated with heat exchangers based solely on natural convection heat transfer.

Various fluid compositions require cooling, either single-phase or multi-phase. For heat exchangers based solely on natural convection, the heat transfer from the cooler tubes (Figure 1) to the surrounding quiescent sea water is generally the limiting factor. Heat transfer from the process fluid inside the tubes to the cooler tubes, and heat transfer through the tube walls have often a smaller thermal resistance than external heat transfer. Therefore, this project aimed to investigate configurations which improve the overall heat transfer, i.e. optimizing the design to enhance the heat transfer from the cooler tubes to the surrounding water, i.e. the external heat transfer.

Weight and size of subsea systems are crucial design parameters. Large structures are more

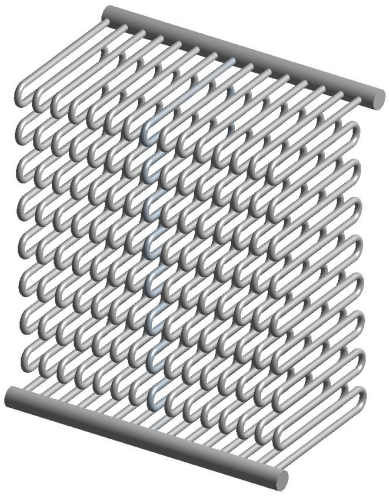

Figure 1: Heat exchanger

expensive and complicated to install, hence subsea components should be designed as small and lightweight as possible without compromising on quality, safety or reliability. Due to its inaccessibility on the seabed, subsea systems must be robust and without need for frequent maintenance.

A subsea heat exchanger may resemble what you find behind your everyday refrigerator, though at a different scale, cf. e.g. Gyles et al. [1] or see Figure 1. A vast amount of design parameters can be varied such as the diameter of the cooler tubes, length, orientation, vertical and horizontal separation distance, number of tubes and so on. This project aimed to get a better understanding of the different mechanisms that contribute to increased or decreased heat transfer from the cooler tubes. Thus, this project has focused on the small scale features associated with subsea heat exchangers. Large scale experiments on a full size heat exchanger is not necessary in order to investigate the small scale features. Experiments on a small part of a subsea heat exchanger will adequately reproduce the features of interest, and was therefore deemed sufficient. As will be discussed more in detail later, experiments on a single cylinder, a pair of cylinders, and an array of three horizontal cylinders were carried out. References to relevant works available in the literature is given in the introduction of the respective papers, thus a long presentation of related work is not given here. In Figure 2 an example of an instantaneous two-dimensional velocity field and temperature field from the experiments is shown, see paper II.

Subsea equipment are generally subjected to ocean currents, which may be of significant importance in heat transfer from subsea heat exchangers. Ocean currents vary with location and time of year, thus the effect of ocean currents on the heat transfer from subsea heat exchangers may vary between applications. However, vertical walls enclosing subsea heat exchangers may be used in order to reduce possible ocean currents effects thus increasing the controllability of the heat exchangers. Hence, ocean currents and similar effects are not considered herein. Only natural convection heat transfer is discussed.

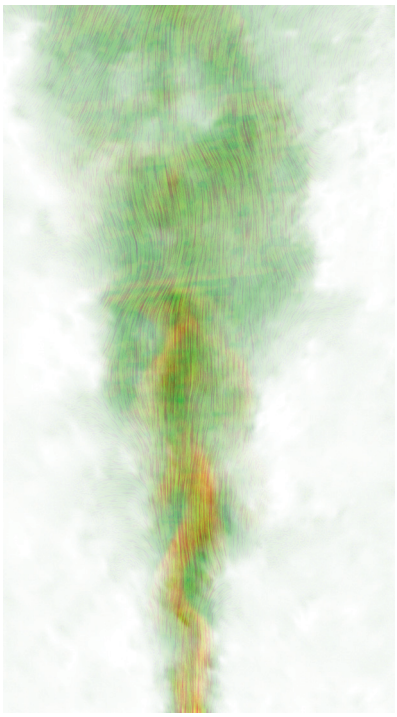

Figure 2: Two-dimensional instantaneous velocity and temperature field above a single unconfined horizontal cylinder under quiescent conditions from measurements. Lines show streamlines, temperature is shown in orange whereas velocity magnitude is visualized by rendering the image using opacity, see paper II.

Computational Fluid Dynamics (CFD) is an important tool in engineering and design of heat exchangers. However, the mainstay engineering approach may not be adequate in design of passive subsea heat exchangers. Natural convection flow associated with subsea heat exchanger possess some flow features which is not adequately predicted using mainstay engineering approaches. CFD-simulations are carried out and compared with experimental results.

Thermal resistances

The overall heat transfer from a heated cylinder may be modeled with the help of a series of thermal resistances, see e.g. Incropera et al. [2]. The radial heat transfer for a circular cylinder is

$$Q_r = \frac{T_b - T_\infty}{\frac{1}{2\pi r_i h_i L} + \frac{ln(r_o/r_i)}{2\pi k L} + \frac{1}{2\pi r_o h_o L}}, \tag{1}$$

where T_b and T_∞ are the process bulk and ambient sea water temperatures respectively. The terms in the denominator are the thermal resistances due to heat transfer from the process fluid to the cooler tube, the thermal resistance due to conductive heat transfer through the pipe wall, and

the thermal resistance due to heat transfer from the cooler tubes to the seawater, respectively. r_i and r_o are inner and outer radii, L is tube length, h is heat transfer coefficient, and k is thermal conductivity of the pipe.

For subsea heat exchangers based solely on natural convection heat transfer, the thermal resistances due to heat transfer from fluids to solids and vice versa is the limiting factor, the thermal resistance due to conduction through the cooler tube wall is generally an order less in magnitude. Thus, the conductivity and thickness of the cooler tubes is of less importance in thermal design of heat exchangers for subsea use. Henceforth the thermal resistances are referred to as the outer, tube and inner resistances.

The inner heat transfer coefficient varies with fluid composition and velocity. For dense process fluids, the inner heat transfer coefficient is generally significantly larger than the outer heat transfer coefficient, thus the outer heat transfer coefficient governs the overall heat transfer. For less dense process fluids, such as dry gases, the inner and outer thermal resistances may be comparable. However, the inner heat transfer coefficient h_i, according to some empirical correlations for the Nusselt number for forced convection within cylinders, is proportional to $V^{4/5}$ where V is the bulk velocity, see Incropera et al. [2]. By designing for a high bulk velocity within the cooler tubes, it is possible to ensure a high inner heat transfer coefficient. Hence, the outer heat transfer coefficient is generally the bottleneck for subsea heat exchangers based solely on natural convection heat transfer.

Fins and other measures to increase the surface area thus increasing external heat transfer are often used in heat exchanger design. However, external fouling on the cooler tubes is a major concern in design of subsea heat exchangers. Fouling may contribute to a significant reduction in the overall efficiency of the heat exchanger. Due to its inaccessibility on the seabed, the use of cooling fins and other measures to increase the outer surface area of the heat exchangers thus improving the overall heat transfer is not an option. Fins may increase the risk of larger fragments attaching to the heat exchanger thus possibly reducing the overall efficiency of the heat exchanger. Furthermore, the use of fins greatly complicates maintenance operations were fouling is physically removed.

Governing equations

Fluid flow is governed by the instantaneous Navier-Stokes equations and mass conservation, whereas heat transfer is governed by the energy equation, cf. e.g. White [3]. Note that in the following Einstein's summation convention is used. The incompressible continuity equation is

$$\frac{\partial u_k}{\partial x_k} = 0, \tag{2}$$

whereas the incompressible Navier-Stokes Equations are

$$\frac{\partial u_i}{\partial t} + u_k \frac{\partial u_i}{\partial x_k} = -\frac{1}{\rho}\frac{\partial p}{\partial x_i} + \frac{\partial}{\partial x_k}(\nu \frac{\partial u_i}{\partial x_k}) + g_i \beta \Delta T, \tag{3}$$

where the Boussinesq approximation has been used, see Gebhart et al. [4]. The Boussinesq approximation is sometimes also referred to as the Boussinesq-Oberbeck approximation as Ober-

beck treated the problem some 20 years before Boussinesq, see Oberbeck [5]. Gray and Giorgini [6] assessed the validity of the Boussinesq-approximation and concluded that the Boussinesq approximation is valid in water as long as $Ra < 10E19$. The Boussinesq-approximation require a density ratio $\Delta\rho/\rho_0$ much less than unity, cf. Gebhart et al. [4]. In water at atmospheric pressure, for the temperature differences herein, the maximum density ratio is 0.015.

The incompressible energy equation as given by e.g. White [3] is

$$\rho C_p(\frac{\partial T}{\partial t} + u_k\frac{\partial T}{\partial x_k}) = \frac{\partial}{\partial x_k}(k\frac{\partial T}{\partial x_k}), \tag{4}$$

Heat is transferred predominantly by convection in fluids, whereas conduction is the sole heat transfer mechanism within solids in a macroscopic sense. Equation (4) describes heat transfer in both solids and fluids. However, for solids the convection term vanishes and the equation describes conductive heat transfer only. The set of equations is able to describe fluid motion and heat transfer in fluids, and heat transfer in solids for arbitrary geometries.

In equations (2), (3) and (4) u is velocity, p is pressure, ρ is density, ν is kinematic viscosity, g is gravity, β is coefficient of thermal expansion, T is temperature, C_p is heat capacity, and k is thermal conductivity.

The Grashof, Rayleigh, Prandtl, and Nusselt numbers and their relevance in buoyant flows

The Grashof number $Gr = \frac{g\beta(T_w - T_\infty)L^3}{\nu^2}$ is a dimensionless number which approximates the ratio of buoyancy forces to viscous forces in a fluid. Subscripts w and ∞ denote wall and ambient conditions respectively, whereas L is a characteristic length scale. By nondimensionalizing the momentum equations (3) and choosing appropriate nondimensional variables, the Grashof number crop up, cf. e.g. Incropera et al. [2]. In natural convective flow the characteristic velocity is often chosen as $U_0 = \sqrt{g\beta(T_w - T_\infty)L}$ which yields the following set of nondimensionalized momentum equations.

$$\frac{\partial u_i^*}{\partial t^*} + u_k^*\frac{\partial u_i^*}{\partial x_k^*} = -\frac{\partial p^*}{\partial x_i^*} + \frac{1}{\sqrt{Gr}}\frac{\partial}{\partial x_k^*}\left(\frac{\partial u_i^*}{\partial x_k^*}\right) + T^* \tag{5}$$

For pure natural convective flow the Grashof number is of equivalent importance in buoyant flow as the Reynolds number is in forced convection. Thus, similarly to high Reynolds number flow, for large Grashof number, the convective term is more dominant than the diffusive term. Furthermore, in natural convection the body force term is the driving force, hence the latter term in equation (5) is imperative. The Nusselt number $Nu = hL/k$ is a dimensionless number which describes heat transfer from solids to fluids. It is a measure of the rate of convective heat transfer over conductive heat transfer in surface heat transfer. For natural convection the Nusselt number is a function of the Grashof and Prandtl number $Nu = f(Gr, Pr)$. Empirical correlations for the Nusselt number for pure natural convection is normally on the form $Nu = CRa^n$, where $Ra = GrPr$ is the Rayleigh number and $Pr = \nu/\alpha$ is the Prandtl number. The thermal diffusivity $\alpha = k/\rho C_p$ is a combination of the material properties in equation (4). The Rayleigh number is a dimensionless number which estimates whether heat transfer primary is

in the form of conduction or convection within a fluid. Below a threshold, heat is transferred mainly by conduction. Equivalent to for large Reynolds numbers, for large Rayleigh numbers the flow is turbulent. Hence, three regimes exist within natural convection; no flow, laminar flow and turbulent flow. Additionally, critical Grashof numbers which suggest whether the flow is laminar or turbulent are available from linear stability theory for plumes and flows adjacent to vertical walls, see e.g. Gebhart et al. [4].

For mixed convection the characteristic velocity is the free stream velocity, hence the nondimensionalized momentum equations become

$$\frac{\partial u_i^*}{\partial t^*} + u_k^* \frac{\partial u_i^*}{\partial x_k^*} = -\frac{\partial p^*}{\partial x_i^*} + \frac{1}{Re}\frac{\partial}{\partial x_k^*}\left(\frac{\partial u_i^*}{\partial x_k^*}\right) + \frac{Gr}{Re^2}T^*. \tag{6}$$

The buoyant term in the latter equations includes the Richardson number $Ri = Gr/Re^2$. When $0.1 < Ri < 10$ both natural and mixed convection is of importance, see e.g. White [3]. Hence, the Nusselt number for mixed convection is on the form $Nu = f(Gr, Re, Pr)$. For large Re, Ri becomes small and buoyant forces is negligible.

Similarly the nondimensionalized energy equation becomes

$$\frac{\partial T^*}{\partial t^*} + u_k^* \frac{\partial T^*}{\partial x_k^*} = \frac{1}{Pe}\frac{\partial}{\partial x_k^*}\left(\frac{\partial T^*}{\partial x_k^*}\right), \tag{7}$$

where $Pe = RePr$ is the Péclet number and is a dimensionless number which describes the rate of advection over diffusion in a fluid, thus it may be of importance in mixed convection, though it is commonly referred to in forced convection only.

Scaling and similarity analysis are important tools in fluid mechanics that may facilitate experimental investigations of large scale features in lab scales given that scaling parameters are available. The Reynolds number play a vital role within a wide range of fields of fluid mechanics. Similarly the Rayleigh and Grashof numbers are of imperative importance in natural convection. Scaled experiments on subsea heat exchangers would enable an investigation of a wide range of features and detailed examination of different geometries. However, the scaling laws for subsea heat exchangers are not easily deducted. As mentioned above, the Nusselt number in natural convection depends on the Rayleigh number only. Moreover, the heat transfer from the upper part of a subsea heat exchanger will be influenced by the flow induced by the lower part of the heat exchanger. Hence, both natural and mixed convection is of importance. The Nusselt number for mixed convection is a function of the Rayleigh number and Reynolds number $Nu = f(Gr, Re, Pr)$. Furthermore, the Reynolds number is proportional to some length scale $Re \sim L$ whereas the Rayleigh and Grashof numbers are proportional to a length scale cubed $Gr \sim Ra \sim L^3$. Thus, it is difficult to build a scaled model of a heat exchanger which satisfies both the Reynolds number and the Grashof or Rayleigh numbers. However, an experimental investigation of a downscaled simple geometry under pure natural convection is possible by compensating for the reduced length scale. For a single horizontal cylinder, a reduction of the diameter with a factor of two would lead to an eightfold increase in temperature to achieve the same Rayleigh number. Scaled experiments in water would quickly lead to practical problems related to high temperatures. To avoid scaling issues, experiments have been carried out with real size geometries, i.e. the diameter of the cooler tubes were chosen similar to those found on subsea heat exchangers.

As briefly mentioned earlier, subsea heat exchangers use seawater as cooling media. Seawater may have different temperature depending on location, depth, time of year and salinity level. For practical reasons, fresh water with a temperature of about 20°C was used in the experiments, though the difference in ambient temperature and salinity level are accounted for in the Rayleigh numbers through the material properties. Thus, a direct comparison with configurations in seawater at the same Rayleigh number is physically sound.

Natural convection from horizontal cylinders, buoyant plumes, instability and turbulence.

Natural convection heat transfer from single horizontal cylinders have been under scrutiny for close to a century. Nusselt [7, 8] introduced the Nusselt number and discussed its applicability related to surface heat transfer from horizontal cylinders under quiescent conditions. Since then, with the introduction of new measurement techniques, analytical or numerical methods, the topic has been revisited a number of times. The contributions by Morgan [9] and Churchill and Chu [10], where they proposed empirical correlations for the Nusselt number $Nu = f(Ra)$ for horizontal cylinders, in addition to the first paper by Nusselt [7], are possibly the most cited papers within the topic. An overview of some of the literature on single horizontal heated cylinders under quiescent conditions is given in papers I and II.

Knowledge about the formation of buoyant plumes above single horizontal cylinders is crucial in heat exchanger design. General solutions for both circular and planar buoyant plumes have been developed by assuming self-similarity, cf. e.g. Gebhart et al. [4]. However, the solutions are only valid for unconfined plumes in the fully turbulent area, or in the purely laminar area for the laminar solutions, and are therefore only applicable in idealized cases, e.g. in the far field from arbitrary sources where inertial forces are negligible. Thermally buoyant plumes rising from point or line sources were first described by Zel'dovich [11] in 1937 according to Hunt and van den Bremer [12] and Gebhart et al. [4]. Morton et al. [13] developed a set of ordinary differential equations for turbulent buoyant plumes by relating the entrainment rate to a characteristic velocity as a closure relation. The ordinary differential equations by Morton et al. [13] are known as the MTT plume conservation equations or MTT model after the authors Morton, Taylor and Turner. See Hunt and van den Bremer [12] for a thorough summary and solution to the MTT equations in addition to a review of the classical plume theory ranging from Zel'dovich to 2010.

Under quiescent conditions, buoyant plumes will form above each of the horizontal tube sections on the lowermost part of the heat exchanger shown in Figure 1. These plumes will interact with the upper part of the heat exchanger. Thus the subsequent interaction between plumes induced from the lowermost tubes with the overlaying tube sections is clearly important on large scale heat exchangers. A number of researchers have investigated the interaction between two or more horizontal cylinders arranged in vertical arrays. The earlier investigations include the work by Liebermann and Gebhart [14] and Marsters [15]. A brief review of some of the existing literature on natural convection from two or more horizontal cylinders is included in paper III and IV.

Turbulent flow generally enhances mixing thus improving heat transfer. A plume under-

going a transition from laminar to turbulent flow will possibly influence the heat transfer of the downstream cooler tubes and hence improve the overall efficiency of a large scale heat exchanger. A planar buoyant plume is statistically homogenous in the spanwise direction. Hence, any spanwise motion is due to redistribution of turbulent kinetic energy. Fluctuations in the spanwise direction is believed to have little influence on the heat transfer from the upper cylinders, lateral and streamwise fluctuations are more important. In paper I a brief discussion around the critical Rayleigh number is given, i.e. the Rayleigh number based on cylinder diameter required to get flow separation from a single cylinder and subsequently a transition to turbulent flow immediately downstream the point of separation.

The stability of buoyant plumes have been scrutinized theoretically and experimentally by several researchers. Both perturbed and unperturbed buoyant plumes have been investigated, cf. e.g. Bill and Gebhart [16], Gebhart et al. [4], and Noto et al. [17]. An overview of some of the relevant literature on the stability of buoyant plumes is given in paper II. Buoyant plumes are far more unstable than buoyant flows adjacent to walls, see Gebhart et al. [4].

As already mentioned, a transition from laminar to turbulent flow will greatly influence the flow characteristics and increase mixing significantly. In pipe flow, where stability theory suggest that the flow is stable to infinitesimal disturbances, it is possible to achieve laminar flow for Reynolds numbers far exceeding the critical Reynolds number in carefully controlled experiments, cf. Hof et al. [18], Eckhardt [19] or Avila et al. [20]. This is not the case for buoyant plumes. Buoyant plumes are unstable to minute perturbations, thus a reliable point of transition should be reproducible, it does not depend on the experimental setup. However, in papers I, II and III Particle Image Velocimetry (PIV) is used to measure instantaneous two-dimensional velocity fields. Particles with a mean diameter of $50\mu m$ were used as flow tracers. The tracer particles may, to some extent, introduce minor disturbances which may trigger transition. The Kolmogorov length scale to tracer particle diameter ratio η/d_p ranged from 4.5 to 2.3 for the Rayleigh numbers under investigation in papers I, II and III, where the Kolmogorov length scale was determined as $\eta = (\nu^3/\varepsilon)^{1/4} = Gr^{-3/8}D$, where D is diameter of the cylinder and ε is dissipation of turbulence kinetic energy and is approximated as $\varepsilon = (g\beta\Delta TD)^{3/2}/D$. However, as earlier discussed, linear stability theory show that infinitesimal perturbations will be amplified in buoyant plumes above a critical Grashof or Rayleigh number. Hence, buoyant plumes are unstable to ever present minute disturbances, thus albeit η/d_p is 2–4, it is improbable that single particles will trigger a transition from laminar to turbulent flow. PIV measurements using smaller particles were not carried out.

Another concern is clustering of particles which may be an issue of special concern in thermal flows. Clusters of particles may introduce perturbations larger than disturbances produced by single particles. During the course of the experiments for various configurations some clustering was observed (visually and in the PIV images), though the amount of clusters were rather small. Clusters had a large effect on the PIV images, thus the water and particles in the test tank was either replaced, or the water was filtered for particles when an unacceptable amount of clustered particles were observed. In order to get a good statistical description of the flow fields a large number of datasets were produced for each configuration. Hence, even though clustered particles hypothetically may influence transition to turbulent flow, it is unlikely that it would influence the statistical description of the flow significantly.

Experimental setup

Experiments were carried out at the Hydrodynamics laboratory at the University of Oslo, Norway, see Figure 3 for pictures from the lab. The experimental setups used in the experiments are described in papers I through IV, with a particular thorough description in paper I. Sketches of the experimental setup is provided in papers I, II, and III, whereas pictures of the setup is given in paper IV. Additional details about measurements and measurement techniques are included below as a supplement to the description given in papers I, II, III, and IV.

Measurements

During this project I have used a number of different measurement techniques for temperature, velocity and heat flux. They include; wall temperature measurements, ambient water temperature measurements, temperature field measurements, three-dimensional point velocity measurements, two-dimensional velocity field measurements and wall heat flux measurements. The measurements were carried out using type k thermocouples, PT100 resistance thermometers, Laser-Induced Fluorescence (LIF), Acoustic Doppler Velocimetry (ADV), Particle Image Velocimetry (PIV), and heat flux sensors respectively.

Velocity measurements

Two-dimensional velocity field measurements were conducted using PIV. The PIV setups are described in papers I, II and III. As briefly mentioned above, tracer particles with a mean diameter of 50 μm were used in the PIV experiments. The particles had a density of $1050\ kg/m^3$, which corresponds to a settling velocity of $u = (\rho_p - \rho)gd_p^2/18\mu = 0.00028\ m/s$, where ρ_d and d_p are density and diameter of the particles, and μ and ρ is molecular viscosity and density of water respectively, see e.g. Douglas et al. [21].

The settling time $\tau_p = \rho_p d_p^2/18\mu$ is small compared to the large scale time scales in buoyant flows, thus the Stokes number $St_T = \tau_p/T_0 =$ where $T_0 = D/U_0$ and $U_0 = \sqrt{g\beta\Delta TD}$ ranges from 0.00007 to 0.00013. However, in order to capture the turbulent characteristics using PIV, the flow tracers must accurately follow the turbulent flow. The Stokes number for the small scales $St_\eta = \tau_p/\tau_\eta$ range from 0.1 to 0.16, where the turbulent time scales are $\tau_\eta = (\nu/\varepsilon)^{1/2} = Gr^{-1/4}D$. In PIV the spatial and temporal resolution of the PIV apparatus determine which frequencies and eddy sizes that are measured. The spatial resolution is larger than the Kolmogorov length scale η, thus the smallest scales are averaged out in the measurements, hence St_η should be sufficiently small to capture the scales detectable by the PIV setup.

In addition to PIV, three–dimensional point velocity measurements using an Acoustic Dopler Velocimeter (ADV) were attempted. The ADV was a Nortek Vectrino with a sampling frequency of 200 Hz. The ADV has an adjustable sampling volume that enables semi non-intrusive time-resolved three-dimensional velocity measurements. However, the buoyant plume above a single cylinder proved difficult to measure using the ADV due to its small size and large velocity gradients. Thus only preliminary measurements were carried out.

Local change of refraction index of water due to temperature gradients may influence PIV measurements. The images may become distorted by refraction of the laser light thus rendering

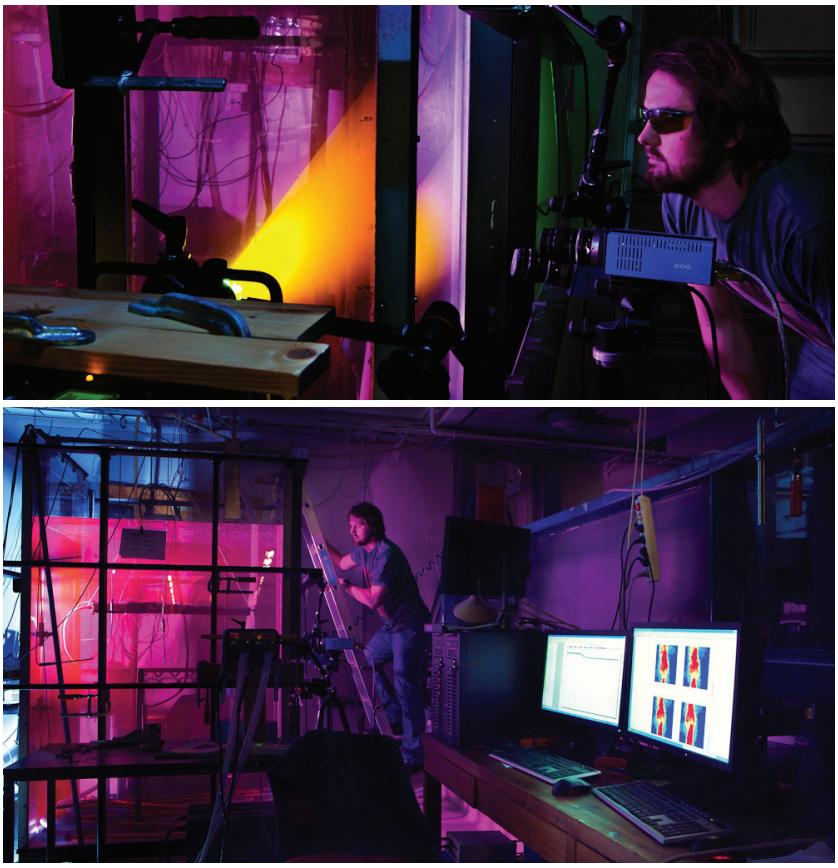

Figure 3: Images of the experiments conducted at the Hydrodynamics laboratory, University of Oslo. The images show the test tank, cameras, computers, lasers and so on used in the experiments, and myself. (Photos:Hans Fredrik Asbjørnsen/UiO)

the images unusable for PIV. An earlier assessment showed that the effect is small far from the source of heat, it is in the same order of magnitude as the noise from the PIV camera, hence it may neglected. However, as slightly discussed in paper I and II, close to the heated cylinder the effect was clearly visible. For this reason, measurements in the distorted region, in close vicinity to the cylinder, was not carried out.

Temperature measurements

Local Nusselt numbers have been determined by temperature measurements on horizontal cylinders in water under quiescent conditions. The Nusselt number were determined by surface and ambient temperature measurements, and the dissipated heat. Thermocouples are small and have a fast response time. Thus they are significantly less intrusive than resistance thermometers and are therefore suited for surface temperature measurements. Thermocouples require two wires of different alloys, an ice-bath reference temperature, and a short circuit at the point of mea-

surement to yield a DC proportional to temperature. The wires in prefabricated thermocouples are generally connected at the tip of a thin housing wire with diameters as small as 0.1 mm. However, the thermocouples must be adjoined to the surface without distorting the temperature and velocity fields in order to measure the surface temperature accurately. Measurements using thin prefabricated thermocouples soldered onto the cylinder surface have proven unsuccessful in earlier investigations. The filler metal greatly influence the heat transfer of the pipe, and distorts the thermal and velocity fields, rendering the approach unusable.

Surface temperature measurements were carried out using type K thermocouples spot welded onto the cylinder surface. Type T thermocouples are more accurate than type K thermocouples. However, type K was chosen because of the alloys weldability to stainless steel. The chromel and alumel alloy wires were flattened to about 0.3 mm and spot welded 3-4 mm apart, creating the short circuit on the cylinder surface rather than within a housing wire. The two wires were oriented downstream the point of measurement to minimize distortion of the temperature and velocity fields. Ambient water temperature was measured using PT100 resistance thermometers. Laser-Induced Fluorescence (LIF) was used to measure the temperature field simultaneously with the velocity field above a heated horizontal cylinder. LIF was chosen over other field temperature measurement techniques due to its similarity with the PIV setup. PIV and LIF may use same type of lighting and cameras. The LIF setup is described in detail in paper II.

Heat flux measurements

Heat flux was attempted measured using heat flux sensors. The Heat Flux sensors are factory calibrated RDF Micro-Foil™ 20453-3 sensors specially made for surface heat flux measurements in water. The sensors are about 11 $mm \times 12$ mm and have a thickness of 0.3 mm. Mounting of sensors in surface heat transfer measurements can be a demanding task. Any intrusive measurement technique may influence the results significantly, therefore, care must be taken in order to avoid distortion of the velocity and temperature fields. Punching grooves in the cylinder surface enables flush mounting of the sensors. However, another issue is of special concern when using surface heat flux sensors in water. Even though the sensor is only 0.3 mm thick and the sensor is flexible, mounting the heat flux sensors to assure perfect heat transfer between the surface and sensor is challenging. Thermal compounds and adhesives are often used to guarantee good thermal contact and to avoid insulating air voids. On curved surfaces, such as a cylinder surface, achieving a good thermal contact is even more demanding.

Preliminary surface heat flux measurements were conducted with a known heat flux on an internally heated cylinder in water using three identical sensors. However, the measurements were far from anticipated. The measured heat flux was significantly less than the actual heat transfer. A twofold increase in actual heat flux yielded about 20-30% increase in measured heat flux for the different sensors. Furthermore, the measured heat flux differed considerably between the sensors as well. The sensors themselves are factory calibrated, hence the measurements are correct. However, the sensors and thermal paste greatly influences the heat transfer characteristics of the cylinder. Most of the heat is transported around the sensor due to the increased thermal resistance. Figure 4 shows a cross section of a pipe with arrows illustrating radial heat transfer. Assuming the temperature on the inner wall of the cylinder is uniform, the heat transfer through the pipe wall can be modeled as

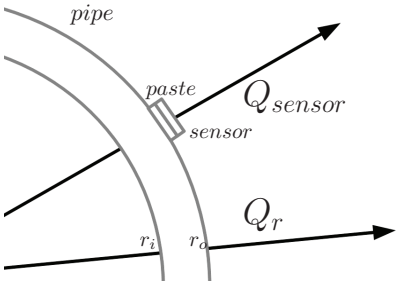

Figure 4: Cross section of pipe with heat flux – not to scale

$$Q_r = \frac{T_{inner\ wall} - T_\infty}{\frac{ln(r_o/r_i)}{2\pi kL} + \frac{1}{2\pi r_o h_o L}}, \tag{8}$$

whereas the heat transfer through the pipe wall, thermal paste and sensor may be modeled as

$$Q_{sensor} = \frac{T_{inner\ wall} - T_\infty}{\frac{ln(r_o/r_i)}{2\pi kL} + \frac{ln((r_o+t_p)/r_o)}{2\pi k_p L} + \frac{ln((r_o+t_p+t_s)/(r_o+t_p))}{2\pi k_s L} + \frac{1}{2\pi(r_o+t_p+t_s)h_o L}}. \tag{9}$$

Subscripts p and s refers to paste and sensor, respectively, whereas t is thickness. For simplicity it is assumed that the outer heat transfer coefficient on the outer surface of the sensor is the same as the outer heat transfer coefficient h_o of the cylinder. An assessment of the thermal resistances show that the thermal resistance through the pipe and sensor is significantly higher than through the pipe wall only, even when assuming a perfect mount of the sensor onto the pipe wall. However, it is still smaller than the thermal resistance due to heat transfer from the cylinder to the water. A significant part of the heat is conducted azimuthally and spanwise within the pipe wall around the sensor and not recorded by the heat flux sensor. In air the heat transfer coefficient is often significantly lower compared to water, hence the thermal resistance due to heat transfer from a cylinder to air is much higher than in water, thus the use of heat flux sensors in air should provide much more accurate data. Some articles are published in the literature using similar sensors for measuring heat flux from horizontal cylinders in water. The published articles all emerge from the same experimental setup consisting of internally heated copper cylinder(s) in water under quiescent conditions. Copper has a thermal conductivity of about 20 times that of stainless steel, hence the sensor will possibly influence the heat transfer at an even greater extent. Although the authors of the mentioned articles recognize the need for calibration techniques to correct the measured heat flux, I strongly believe that the use of such sensors for the present application should be avoided. I believe the sensor influence the heat transfer to such an extent that the experimental setup is invalid. However, if the cylinder is coated in a material with similar thermal characteristics as the heat flux sensor, and a good thermal contact between the sensor and cylinder is achieved, the use of heat flux sensors similar to the present may be used in surface heat flux measurements of metallic cylinders in water.

I originally planned to use heat flux sensors to measure heat flux and wall temperatures to estimate the local Nusselt numbers. However, due to the problems described above, heat flux measurements were not carried out, other than the preliminary measurements.

Computational Fluid Dynamics

Computational Fluid Dynamics (CFD) have been used as a design tool for subsea systems for a long time. However, in general, many engineers tend to have an overly confidence in the CFD-tools and their applicability. It exists a vast amount of models and closure relations that accounts for turbulent effects that makes turbulent simulations feasible on an engineering level. Certain models work great for specific types of flow, but breaks down for other types. The celebrated $k-\varepsilon$ model e.g. performs well for pipe flow and many other types of flow, but fails to predict separation over an airfoil or in a pipe bend, see e.g. Menter et al. [22]. Furthermore, models are often used for other types of flow than intended, without experimental validation, nor without comparison with other models. However, simulations are often carried out with a relatively large safety margin and often with rather conservative input data. Such an approach will provide ballpark results, which in some cases is adequate in engineering. Another pitfall encountered in modern commercial CFD-codes is the use of wall-functions. Wall-functions enables for high Reynolds number simulations without the need for a fully resolved boundary layer. However, in general, wall-functions are developed for high Reynolds number flow only, but are applied to other types of flow by unaware CFD-users. Thus wrongly applied wall functions may significantly influence the results yielding totally unphysical results.

CFD-results are often easily accessible and are able to provide results in a fraction of a time compared to elaborate experiments. Moreover, the results often look physical plausible, but may very well be totally wrong due to model failure or false input. Without experimental validation or any quantitative knowledge of the flow field, significant errors may be overlooked. Modern commercial CFD-codes are very forgiving, meaning that unphysical input may result in a converged solution. CFD is widely used not only in engineering, but also in fundamental research in fluid mechanics, in turbulence research in particular.

Reynolds Averaged Navier-Stokes – RANS

In buoyant incompressible RANS simulations, ensemble averaged versions of the continuity equation (2), momentum equations (3), and the energy equations (4) are solved, see e.g. White [3]. The ensemble averaged continuity equation is

$$\frac{\partial U_k}{\partial x_k} = 0, \tag{10}$$

the incompressible ensemble averaged momentum equations are

$$\frac{\partial U_i}{\partial t} + U_k \frac{\partial U_i}{\partial x_k} = -\frac{1}{\rho}\frac{\partial P}{\partial x_i} + \frac{\partial}{\partial x_k}\left(\nu \frac{\partial U_i}{\partial x_k}\right) + g_i \beta \Delta T - \frac{\partial \overline{u_i' u_k'}}{\partial x_k}, \tag{11}$$

and the ensemble averaged energy equation is

$$\frac{\partial T}{\partial t} + U_k \frac{\partial T}{\partial x_k} = \frac{\partial}{\partial x_k}(\alpha \frac{\partial T}{\partial x_k}) - \frac{\partial \overline{u_k' t'}}{\partial x_k}. \tag{12}$$

The variables in equations equations (2), (3), and (4) are decomposed using Reynolds decomposition $u_i = U_i + u_i'$, thus U_i T, and P are ensemble averaged quantities, whereas u_i', p', and t'

are fluctuating components, see e.g. White [3]. The Reynolds stresses $\overline{u_i' u_j'}$ and turbulent fluxes $\overline{u_i' t'}$ in equations (11) and (12) require modeling to close the set of equations, overbar denotes the ensemble average. Two-equation single point RANS closure-models, such as the $k-\varepsilon$ and Shear-Stress Transport (SST) models rely on a linear eddy viscosity model which relates the Reynolds stresses to a turbulent viscosity cf. e.g. Durbin and Reif [23].

$$-\overline{u_i' u_j'} = 2\nu_t S_{ij} - 2/3k\delta_{ij} \tag{13}$$

$S_{ij} = \frac{1}{2}(\frac{\partial U_i}{\partial x_j} + \frac{\partial U_j}{\partial x_i})$ is the mean rate-of-strain-tensor, $k = \frac{1}{2}(\overline{u'^2} + \overline{v'^2} + \overline{w'^2})$ is turbulent kinetic energy and ε is dissipation of turbulent kinetic energy. In the $k-\varepsilon$ model and other similar models, in addition to the ensemble averaged continuity equation (10), the RANS equations (11), and energy equation (12), two transport equations for k and ε are solved.

The turbulence is modeled using a single scalar ν_t, which for a $k-\varepsilon$ model is $\nu_t = C_\mu k^2/\varepsilon$, where C_μ is a constant, see e.g. Durbin and Reif [23]. Hence, the turbulence is inherently assumed to be isotropic which in flows subjected to body forces or even in boundary layers is not the case, cf. Hanjalić [24]. Another major assumption is that it assumes an equilibrium between Reynolds stresses and the mean rate-of-strain. The latter assumption is sound for many types of turbulent flow, but is inherently wrong for free shear flows, flows with strong anisotropy, buoyant flows, and secondary flows, see e.g. Durbin and Reif [23] and ANSYS [25]. The turbulent fluxes $\overline{u_i' t'}$ are often modeled analogously to the eddy viscosity using an eddy diffusivity $\alpha_t = \frac{\nu_t}{Pr_t}$, where Pr_t is turbulent Prandtl number. The turbulent fluxes are often modeled using $\overline{u_i' t'} = -\alpha_t \frac{\partial T}{\partial x_i}$.

A more physical sound approach which overcomes many of deficiencies associated with the linear eddy viscosity model is the use of second moment transport models (Reynolds stress models – RSM) which includes transport equations for the Reynolds stresses $\overline{u_i' u_j'}$. Transport equations are solved for the Reynolds stresses $\overline{u_i' u_j'}$ instead of using the linear stress-strain relation (equation (13)) and solving a single equation for turbulent kinetic energy k, cf. e.g. Hanjalić [24]. Reynolds stress models offer a considerable potential for further improved modeling of complex flow phenomena. However, according to Hanjalić [24] the transport equations for $\overline{u_i' u_j'}$ contain a considerable amount of terms which require modeling. Hence, the RSM does not necessarily outperform the simpler eddy viscosity models for simple flows. Nevertheless, the RSM may emulate buoyant turbulent flow better than linear eddy viscosity models.

In many engineering applications the flow is always fully turbulent. However, for natural convection heat transfer this is not the case, even for large bulk Rayleigh numbers it is common to encounter both laminar, transitional and turbulent flow – all in one flow, see Hanjalić [24]. For natural convection heat transfer from a horizontal cylinder under quiescent conditions the flow around the lower part of the cylinder will be laminar even for very high Rayleigh numbers ($Ra \lesssim 10E11$), see e.g. Kitamura et al. [26]. Within the buoyant plume far downstream the heated cylinder and far from solid boundaries the plume is likely to undergo a transition from laminar to turbulent flow even for low Rayleigh numbers ($Ra \gtrsim 1$) based on cylinder diameter, see Noto et al. [17]. Thus, in natural convection heat transfer from horizontal cylinders both laminar and turbulent flow is of importance. RANS-models are developed for purely turbulent flow, hence they are generally unable to predict a laminar to turbulent transition.

Turbulence models are developed for fully turbulent conditions and calibrated against tur-

bulence data, thus without considering the laminar to turbulent transition problem, it is unlikely that low intensity turbulent flow is accurately predicted by RANS models.

Large-Eddy Simulations – LES

Even though Large Eddy Simulations (LES) have been around for many years, and the available computational power has increased at a blistering pace making LES feasible for may applications, RANS-modeling is still the mainstay in engineering. LES is a more elaborate compared to RANS simulations, though some LES models are able to capture laminar to turbulent transition processes and other features which generally are not tractable by RANS-models, see Pope [27].

In LES, as the name implies, the larger three-dimensional motions are directly represented whereas the small scale effects, i.e. the effects smaller than the computational grid, are modeled. Thus the amount of turbulent kinetic energy that is modeled is determined by the computational grid, cf. e.g. Pope [27]. Hence, contradictory to RANS where all effects of turbulent motion are modeled, LES is grid dependent. However, if sufficiently resolved, statistical grid independence is achieved.

In LES spatial filtered versions of the continuity equation (2),

$$\frac{\partial \tilde{U}_k}{\partial x_k} = 0, \tag{14}$$

the incompressible Navier-Stokes equations (3),

$$\frac{\partial \tilde{U}_i}{\partial t} + \tilde{U}_k \frac{\partial \tilde{U}_i}{\partial x_k} = -\frac{1}{\rho}\frac{\partial \tilde{P}}{\partial x_i} + \frac{\partial}{\partial x_k}(\nu \frac{\partial \tilde{U}_i}{\partial x_k}) + g_i \beta \Delta \tilde{T} - \frac{\partial \tau_{ij}}{\partial x_j}. \tag{15}$$

and the energy equation (4) are solved

$$\frac{\partial \tilde{T}}{\partial t} + \tilde{U}_k \frac{\partial \tilde{T}}{\partial x_k} = \frac{\partial}{\partial x_k}(\alpha \frac{\partial \tilde{T}}{\partial x_k}) - \frac{\partial q_k}{\partial x_k}. \tag{16}$$

Here $\sim$ denotes low-pass filtered quantities such as the filtered velocity $\tilde{U}_i$, cf. Pope [27]. The latter terms in equations (15) and (16) include the unresolved stress term tensor $\tau_{ij} = \widetilde{u_i u_j} - \tilde{u}_i \tilde{u}_j$ and the unresolved turbulent fluxes $q_i = \widetilde{u_i t} - \tilde{u}_i \tilde{t}$ which both require modeling. In LES models a linear eddy viscosity is often used as a relation between the residual stresses τ_{ij} and the filtered rate of strain $\tilde{S}_{ij} = \frac{1}{2}(\frac{\partial \tilde{U}_i}{\partial x_j} + \frac{\partial \tilde{U}_j}{\partial x_i})$, see e.g. Pope [27].

$$\tau_{ij} - 1/3 \tau_{kk} \delta_{ij} = -2\nu_t \tilde{S}_{ij} \tag{17}$$

Similarly to turbulence models with scalar variables in RANS-modeling, the use of equation (17) impose isotropicity. However, in LES only the unresolved scales are isotropic, the direct representation of larger energetic eddies facilitates anisotropicity on a larger scale. Anisotropic turbulence is important in turbulent flows with body forces such as buoyancy. In buoyant turbulent plumes the effect of body forces on turbulence largely enters through mean shear, the direct effect of buoyancy on turbulence is less pronounced, see Shabbir and George [28] or paper I. Various models for the eddy viscosity ν_t exists in the literature. The classical Smagorinsky

model is probably the most utilized model within LES. The scalar eddy viscosity is related to the filtered rate of strain $\nu_t = (C_s\Delta)^2\tilde{S}_{ij}$, see Pope [27]. C_s is the Smagorinsky constant which in the original model is a constant. In later approaches, such as the dynamic Smagorinsky model introduced by Germano et al. [29], the model coefficient is computed based on local variables which allows for laminar to turbulent transitions and reversed energy transfer from small to larger scales. One of the shortcomings of the original Smagorinsky model for transitional flows was its dissipative nature, the constant coefficient led to an extensive dampening of resolved structures due to the increased total viscosity, see Germano et al. [29]. An elevated total viscosity will dampen out perturbations thus preventing correct predictions of the transition process. The dynamic Smagorinsky model was introduced to overcome this and other deficiencies of the original model, see Germano et al. [29]. Furthermore, reversed energy transfer may be accounted for in the dynamic procedure through a negative model coefficient which reduces the effect of diffusion in the filtered momentum equations. In order to accurately predict laminar to turbulence transitions, it is vital that the subgrid model correctly reflects the state of the flow, thus yielding appropriate model coefficients which enables initial disturbances to grow at a correct rate, and accurately accounts for turbulent effects in the fully turbulent region.

Direct Numerical Simulations – DNS

In direct numerical simulations the continuity equation (2), the Navier-Stokes equations (3) and the energy equation (4) are solved directly, modeling is not required. DNS require temporal and spatial resolution of the entire range of scales, from the smallest dissipative scale to the largest integral scale, cf. Pope [27]. As briefly mentioned earlier, DNS is used in turbulence research. DNS facilitates whole field investigations of all spatial and temporal scales in turbulent flows, which generally is not possible in experiments. However, the computational cost of a DNS can be imense, the computational cost of a DNS, according to Pope [27], scales with $Ra^{9/4}$. Thus DNS of real flows is extremely time consuming and is chiefly not possible for real flows even with a supercomputer at hand. Furthermore, DNS provide data about all scales in a turbulent flow, which from an engineering point of view would quickly lead to an overflow of information. Hence, in cases where RANS or LES yields accurate data, DNS is prohibitively extensive for all other reasons than turbulence research. DNS is not attempted during this project.

Papers summary

The main body of this thesis consist of six journal papers. A brief summary of the published and submitted papers is given below.

As previously mentioned some of the small scale features associated with large scale subsea heat exchangers were investigated. Particularly the mechanisms that contribute to increased or decreased heat transfer from the cooler tubes were scrutinized. The velocity field above a single cylinder may yield important design criteria for heat exchangers based solely on natural convection heat transfer, thus an experimental investigations of the buoyant plume forming above a single cylinder were carried out in paper I and paper II. The interaction between cooler tubes, i.e. the effect of the impinging plume induced from the lowermost cooler tube on the second tube, may improve the heat transfer. Hence, an experimental investigation of two vertically

arranged horizontal cylinders were carried out in paper III. Moreover, the separation distance between the subsequent cooler tubes, for a subsea heat exchanger similar to the illustration in Figure 1, does not necessarily have to be the same between all cooler tubes to exploit the effects found in papers I, II and III. Thus an experimental investigation of three vertically arranged horizontal cylinders were carried out in paper IV.

CFD is an important tool in design of heat exchangers. However, natural convection flow possess some features which are not easily captured by conventional engineering CFD simulations. Thus LES of a single heated horizontal cylinder are carried out in paper V and compared with experimental results from paper I and II.

Furthermore, in engineering approximate results are often adequate, and LES-codes are often not available. Thus RANS simulations with general purpose CFD-tools and comparison against experimental results are therefore carried out in paper VI.

Paper I – PIV investigation of buoyant plume from natural convection heat transfer above a horizontal heated cylinder

The first paper entitled "PIV investigation of buoyant plume from natural convection heat transfer above a horizontal heated cylinder" is an experimental investigation of the velocity field above an uniformly heated horizontal cylinder. The circumferential Nusselt number was also scrutinized for Rayleigh numbers ranging from $2.05E7$ to $7.94E7$. The instantaneous two-dimensional velocity field above the cylinder was measured using PIV. Statistical descriptions of the mean and fluctuating velocity fields were given based on 6400 instantaneous velocity fields. The results show that the plume undergoes a transition from laminar to turbulent flow downstream the cylinder. The mean velocity fields were compared to similarity solutions for buoyant turbulent plumes and compares well in the turbulent region. As mentioned earlier only preliminary ADV measurements were carried out, hence the spanwise velocity component was not measured. However, the ADV results clearly showed that there was a spanwise velocity component a distance downstream the cylinder for the various Rayleigh numbers.

The similarity solution for turbulent buoyant plumes is according to Gebhart et al. [4] $\bar{V} = k_2 B_0^{1/3} \exp^{(-32\frac{x^2}{y^2})}$. The expression is derived from dimensional similarity considerations and compared to experiments in the purely buoyant region for buoyant jets. In paper I the velocity approximation $k_2 B_0^{1/3}$ was not given much attention because the buoyant flux B_0, as it is given by Gebhart et al. [4], is a function of the jet outlet velocity. However, the buoyant flux may be approximated using the heat flux rather than the jet orifice velocity. The buoyant flux is $B_0 = \frac{g\beta Q}{\rho C_p}$, where Q is dissipated heat per length $[W/m]$. $k_2 B_0^{1/3}$ yields plume center velocities of 11.2, 14.1 and 16.1 mm/s whereas the measured values were 13.5, 14.4 and 18.5 mm/s respectively. $k_2 = 1.66$ is an experimentally determined constant according to Gebhart et al. [4]. The plume center velocity was initially large close to the cylinder, but decreases in the transitional region before reaching a constant value in the turbulent region. The transition from laminar to turbulent flow is an important feature which may influence design of heat exchangers considerably.

Unfortunately, some errors have found their way into paper I. In equation (4), the diffusive term in the momentum equations was written as $\nu\partial_{jj}U_i$. However, the correct notation is $\nu\partial^2_{jj}U_i$.

For the expression for the turbulent similarity solution given in paper I $\bar{V} = k_2 B_0^{1/3} \exp^{(-32\eta_0)}$, another error emerged. The correct expression is $\bar{V} = k_2 B_0^{1/3} \exp^{(-32\eta_0^2)}$ where $\eta_0 = x/y$.

Furthermore, the production of turbulent kinetic energy was given some attention in paper I. However, I later realized that the estimate of turbulent kinetic energy in paper I is not entirely correct. The estimates for correlations $\overline{u^2}$, $\overline{v^2}$, and $\overline{uv}$, presented in the paper, are influenced by a shedding motion. A separation of the turbulent motion from the shedding motion is required to accurately assess the production of turbulent kinetic energy. This is also the case for the discussion on production of turbulent kinetic energy due to mean shear and due to buoyancy in paper II.

Paper II – Simultaneous PIV/LIF measurements of a transitional buoyant plume above a horizontal cylinder

The second paper entitled "Simultaneous PIV/LIF measurements of a transitional buoyant plume above a horizontal cylinder" contains the results from simultaneous temperature and velocity field measurements above a single heated horizontal cylinder with $Ra = 9.4E7$. Knowledge about the developing temperature field may yield additional knowledge about the developing buoyant plume above a heated horizontal cylinder. The velocity and temperature fields were measured above an evenly heated horizontal cylinder using PIV and LIF. The temperature and two-dimensional velocity fields were measured simultaneously to get a complete picture of the production of turbulent kinetic energy and the temperature field in addition to the previously measured velocity field. A relatively detailed description of the LIF post-processing was given as it differs slightly from what is available in the literature. The results showed, similarly to paper I, that the plume undergoes a transition from laminar to turbulent flow a distance downstream the cylinder. The transition onset moved further upstream towards the cylinder compared to the results in paper I. Unfortunately, an error cropped up paper I as well. In equation (7), the diffusive term was written as $\nu \frac{\partial U_i}{\partial x_j \partial x_j}$, the correct notation is $\nu \frac{\partial^2 U_i}{\partial x_j \partial x_j}$.

Paper III – Natural convection heat transfer from two horizontal cylinders at high Rayleigh numbers

In the third paper entitled "Natural convection heat transfer from two horizontal cylinders at high Rayleigh numbers", the interaction between two vertically arranged horizontal cylinders was investigated. The induced plume from the lowermost cylinder will greatly influence the heat transfer from the upper cylinder. In the literature two counteracting effects are identified that will alter the heat transfer from the upper cylinder, namely reduced heat transfer due to increased ambient temperature and increased heat transfer due to the induced velocity field. Five different separation distances S and seven different Rayleigh numbers ranging from $Ra = 1.82E7$ to $Ra = 2.55E8$ were investigated. The effect of a transitional or turbulent plume impinging on the upper cylinder was thoroughly discussed in paper III. The change in local Nusselt number compared to the single unbounded cylinder was discussed, and the velocity field above the second cylinder was measured using PIV. The ensemble averaged velocity fields above the second cylinder was compared to the single cylinder. The results showed that a

considerable gain in Nusselt number was achieved by increasing the separation length slightly ($0.5D$). However, a further increase does not increase the Nusselt number much.

Paper IV – Natural convection heat transfer from three vertically arranged horizontal cylinders with dissimilar separation distance

The fourth paper consider natural convection heat transfer from three vertically arranged horizontal cylinders under quiescent conditions for $Ra = 1.96E7$ and $5.35E7$. The distance between the cylinders were varied from $2D$ to $5D$. The effect turbulence has on the heat transfer on the upper cylinders in the array was discussed and the effect of dissimilar cylinder spacings between the cylinders was investigated. The effect of reducing the distance between the two upper cylinders compared to the distance between the lower cylinders have been given much attention. The results generally show, for the investigated separation distances and Rayleigh numbers, that the distance between the two upper cylinders may be less than the two lower cylinders. Hence, a dissimilar cylinder separation distance may be beneficial both for increasing the overall efficiency of the heat exchanger and in order to minimize its sheer size.

Paper V – Large eddy simulations of a buoyant plume above a heated horizontal cylinder at intermediate Rayleigh numbers

In paper V LES simulations of a horizontal cylinder was carried out and compared with the experimental results from paper I and II. LES with the dynamic Smagorinsky subgrid stress model were carried out. The results show that the LES was able to predict a transition from laminar to turbulent flow without any form of triggering, the flow develops from a laminar flow into a turbulent flow downstream the cylinder. However, even though the first perturbations occur at about the same location as in the experiments, the plume growth was underpredicted in the simulations. The plume half-width was significantly narrower than in the experimental investigation.

An assessment of the performance of the subgrid model was not carried out, other than a comparison with experimental data, but the results suggests that the model is unable to adequately emulate the laminar to turbulent transition process. The results indicate that the deficiencies from the original model, to some extent, crop up here, i.e. the turbulence eddy viscosity ν_t prevent a correct growth rate of the initial perturbations.

Paper VI – Unsteady RANS simulations of a buoyant plume above a cylinder

The sixth paper, entitled ”Unsteady RANS simulations of a buoyant plume above a cylinder“ was more of an engineering approach. As the title implies, URANS simulations of a buoyant plume above a heated horizontal cylinder was carried out using CFX, a commercially available general purpose CFD-tool. As earlier discussed, the rather simple problem of natural convection heat transfer from a single cylinder possess some difficulties which hardly is amendable by RANS-modeling. However, in engineering, LES may not be feasible or it may be considered

to elaborate for engineering applications. Hence, RANS-simulations with comparison against experimental results were carried out.

Bibliography

[1] B.R. Gyles, B. Hægland, T.B. Dahl, A. Sanchis, S. Grafsrønningen, R.B. Schüller, and A. Jensen. Natural convection - subsea cooling; theory, simulations, experiments and design. *Proceedings of the ASME 30th International Conference on Ocean, Offshore and Arctic Engineering*, 2011.

[2] F.P. Incropera, D.P. DeWitt, T.L. Bergman, and A.S. Lavine. *Fundamentals of Heat and Mass Transfer*. John Wiley and Sons Inc., 2007.

[3] F.M.White. *Viscous Fluid Flow*. McGraw-Hill International Editions, 1991.

[4] B. Gebhart, Y. Jaluria, R.L. Mahajan, and B. Sammakia. *Buoyancy-induced flows and transport*. Hemisphere Publishing Corporation, 1988.

[5] A. Oberbeck. Über die Wärmeleitung der Flüssigkeiten bei Berücksichtigung der Strömungen infolge von Temperaturdifferenzen. *Annalen der Physik*, 243(6):271–292, 1879.

[6] D.D. Gray and A. Giorgini. The validity of the Boussinesq approximation for liquids and gases. *International Journal of Heat and Mass Transfer*, 19:545–551, 1976.

[7] W. Nusselt. Das Grundgesetz des Wärmeüberganges. *Gesundheitsingenieur*, 38:477–482, 1915.

[8] W. Nusselt. Die Wärmeabgabe eines waagrecht liegenden Drahtes oder Rohres in Flüssigketein und Gasen. *Zeitschrift des Vereines deutscher Ingenieure*, 41:1475–1478, 1929.

[9] V.T. Morgan. The overall convective heat transfer from smooth circular cylinders. *Advances in heat transfer*, 11:199–264, 1975.

[10] S.W. Churchill and H.H.S. Chu. Correlating equations for laminar and turbulent free convection from a horizontal cylinder. *International Journal of Heat and Mass Transfer*, 18:1049–1053, 1975.

[11] Y.B. Zeldovich. The asymptotic laws of freely-ascending convective flows. *Zh. Eksp. Teor. Fiz*, 7:1463–1465, 1937 (in Russian) English translation in *Selected Works of Yakov Borisovich Zeldovich*, 1:82–85, 1992 (J.P. Ostriker ed.), Princeton University Press.

[12] G.R. Hunt and T.S. van den Bremer. Classical plume theory 1937-2010 and beyond. *IMA Journal of Applied Mathematics*, pages 424–448, 2010.

[13] B.R. Morton, G. Taylor, and J.S. Turner. Turbulent gravitational convection from maintained and instantaneous sources. *Proceedings of the Royal Society of London. Series A, Mathematical and Physical Sciences*, 234:1–23, 1956.

[14] J. Lieberman and B. Gebhart. Interactions in natural convection from an array of heated elements, experimental. *International Journal of Heat and Mass Transfer*, 12:1385–1396, 1969.

[15] G.F. Marsters. Arrays of heated horizontal cylinders in natural convection. *International Communications in Heat and Mass Transfer Journal of Heat and Mass Transfer*, 15:921–933, 1972.

[16] R.G. Bill and B. Gebhart. The transition of planar plumes. *International Journal of Heat Mass and Transfer*, 18:513–526, 1975.

[17] K. Noto, K. Teramoto, and T. Nakajima. Spectra and critical Grashof numbers for turbulent transition in a thermal plume. *Journal of Thermophysics and Heat Transfer*, 13:82–90, 1999.

[18] B. Hof, C. W.H. van Doorne, J. Westerweel, F.T.M. Nieuwstadt, H. Faisst, B. Eckhardt, H. Wedin, R. R. Kerswell, and F. Waleffe. Experimental observation of nonlinear traveling waves in turbulent pipe flow. *Science*, 305:1594–1598, 2004.

[19] B. Eckhardt. A critical point for turbulence. *Science*, 333:165–166, 2011.

[20] K. Avila, D. Moxey, A. de Lozar, M. Avila, D. Barkley, and B. Hof. The onset of turbulence in pipe flow. *Science*, 333:192–196, 2011.

[21] J.F. Douglas, J.M. Gasiorek, and J.A. Swaffield. *Fluid Mechanics*. Prentice Hall, 2001.

[22] F.R. Menter, M. Kuntz, and R. Langtry. Ten years of industrial experience with the sst turbulence model. *Turbulence Heat and Mass Transfer 4*, 4:2003, 2003.

[23] P.A.Durbin and B.A.Pettersson Reif. *Statistical theory and modeling for turbulent flows*. John Wiley and Sons Inc., 2003.

[24] K. Hanjalić. One-point closure models for buoyancy driven turbulent flows. *Annual Review of Fluid Mechanics*, 34:321–347, 2002.

[25] ANSYS Inc. *ANSYS CFX-Solver Modeling guide*, release 12.0 edition, April 2009.

[26] K. Kitamura, F.Kami-iwa, and T. Misumi. Heat transfer and fluid flow of natural convection around large horizontal cylinders. *International Journal of Heat and Mass Transfer*, 42:4093–4106, 1999.

[27] S.B. Pope. *Turbulent flows*. Camebridge University Press, 2000.

[28] A. Shabbir and W.K. George. Experiments on a round turbulent buoyant plume. *Journal of Fluid Dynamics*, 275:1–32, 1994.

[29] M. Germano, U. Piomelli, P. Moin, and W.H. Cabot. A dynamic subgridscale eddy viscosity model. *Phys. Fluids A*, pages 1760–1765, 1991.

Papers

Paper I **Grafsrønningen S., Jensen A. & Reif. B.A.P.** 2011
PIV investigation of buoyant plume from natural convection heat transfer above a horizontal heated cylinder
International Journal of Heat and Mass Transfer **54**, 4975–4987.

Paper II **Grafsrønningen S. & Jensen A.** 2012
Simultaneous PIV/LIF measurements of a transitional buoyant plume above a horizontal cylinder
International Journal of Heat and Mass Transfer **55**, 4195–4206.

Paper III **Grafsrønningen S. & Jensen A.** 2012
Natural convection heat transfer from two horizontal cylinders at high Rayleigh numbers
International Journal of Heat and Mass Transfer **55**, 5552–5564.

Paper IV **Grafsrønningen S. & Jensen A.** 2013
Natural convection heat transfer from three vertically arranged horizontal cylinders with dissimilar separation distance at intermediate Rayleigh numbers
International Journal of Heat and Mass Transfer **57**, 519–527

Paper V **Grafsrønningen S., Jensen A. & Reif. B.A.P.** 2012
Large eddy simulations of a buoyant plume above a heated horizontal cylinder at intermediate Rayleigh numbers
Submitted to International Journal of Heat and Mass Transfer

Paper IV **Grafsrønningen S. & Jensen A.** 2012
Unsteady RANS simulations of a buoyant plume above a cylinder
Submitted to Engineering and Computational Mechanics

Paper I

PIV investigation of buoyant plume from natural convection heat transfer above a horizontal heated cylinder

Paper II

Simultaneous PIV/LIF measurements of a transitional buoyant plume above a horizontal cylinder

Paper III

Natural convection heat transfer from two horizontal cylinders at high Rayleigh numbers.

Paper IV

Natural convection heat transfer from three vertically arranged horizontal cylinders with dissimilar separation distance at intermediate Rayeligh numbers

Paper V

Large eddy simulations of a buoyant plume above a heated horizontal cylinder at intermediate Rayleigh numbers

Paper VI

Unsteady RANS simulations of a buoyant plume above a cylinder

Unsteady RANS simulations of a buoyant plume above a cylinder

Stig Grafsrønningen*+ & Atle Jensen*

Unsteady RANS simulations of a horizontal heated cylinder with $Ra = 9.4E7$ is carried out and compared with experimental data of a heated horizontal cylinder with a diameter of 54mm in water. Different one-point closure models were used, both two-equation turbulence models, and more sophisticated Reynolds stress models. Simulations with models relying on the ε-equation which use wall-functions to predict wall heat flux proved erroneous. The wall-functions underestimate the wall heat flux from the cylinder with factors of more than 20 depending on the model. Simulations with models which combine the best features of the eddy frequency ω-formulations and turbulent kinetic energy dissipation ε-formulations gave significantly better results.

Natural convection heat transfer from horizontal cylinder at intermediate Rayleigh numbers involve a laminar to turbulent transition downstream the heated cylinder. Such features are generally not tractable by RANS models. The results approach the laminar solution regardless of the model used, thus turbulent effects which crop up downstream the cylinder are not captured and the ensemble averaged results differ significantly with the experimental results.

Nevertheless, the simulations are examples of mainstay engineering approaches, and illustrates possible problems and pitfalls when using commercial general purpose CFD codes without comparison against experimental results nor other means of verification. Natural convection heat transfer from a single horizontal cylinder at intermediate Rayleigh numbers is a well examined classical problem within heat transfer research. However, even though the geometry is very simple, the problem involve rather complex flow features which is hardly amendable by RANS or even LES.

Submitted to Engineering and Computational Mechanics 21 September 2012

* *Mechanics Division, Department of Mathematics, University of Oslo (UiO), P.O. Box 1053, Blindern, NO-0316 Oslo, Norway*
+ *Corresponding author, +47 95 19 11 83, stig@math.uio.no*

Introduction

Computational Fluid Dynamics (CFD) is widely used in a number of engineering branches. CFD may fascilitate performance testing of complex heat exchanger designs without the need for multiple physical models, or complex test facilities. Design changes may be incorporated and tested quicker and cheaper than in extensive experimental testing. Detailed knowledge about unmeasureable quantities is easily accessible in CFD. Drag, heat transfer characteristics and other important variables are relatively quickly obtainable in CFD, depending on the type of simulation, geometry and so on. Furthermore, in the oil industry there is an increasing demand for detailed analysis of various equipment during different operating procedures. Hydrate formation is a major concern in design of subsea equipment and in daily production of oil and gas from subsea fields. Hydrates may form in areas with high pressure, low temperature, free water and natural gas, i.e. conditions typically encountered within subsea equipment after a shut down of production from subsea gas fields. Thus, heat transfer problems, natural convection in particular, is of great significance. Herein natural convection heat transfer related to subsea heat exchangers is scrutinized. However, the results are of equal importance and validity for other configurations where natural convection is encountered.

CFD is largely divided into Direct Numerical Simulations (DNS), Large Eddy Simulations (LES) and Reynolds Averaged Navier-Stokes simulations (RANS). In DNS the whole range of scales must be resolved, both spatially and temporally, from the smallest dissipative scales to the integral scale. DNS is far from becoming feasible in engineering even with the development of computational resources seen lately. LES and RANS rely on turbulence modeling in order to make turbulent simulations feasible and to close the set of equations. In LES a set of instantaneous filtered Navier-Stokes equations are solved where the turbulent scales smaller than the grid size are modelled. In RANS-simulations all of the turbulent effects are modeled. LES is more elaborate than RANS-simulations, though LES may provide information about the turbulence. A set of instantaneous equations are solved, and averaging is necessary in order to get a statistical description of the variables. In RANS a set of ensemble averaged equations is solved yielding the ensemble averaged results.

However, CFD has its limitations. As mentioned, CFD in engineering rely on closure models to account for turbulent effects. Many of the models have proven to work great for a wide range of different flows. However, for certain flows, many of the models break down. Simulations with inappropriate closure models may yield physical looking, yet totally wrong results which may be overlooked without an $a\ priori$ knowledge about the flow field nor experimental results or other means of verification.

Natural convection heat transfer from horizontal cylinders at moderate Rayleigh numbers involves a transition from laminar to turbulent flow downstream the cylinder, see e.g. Grafsrønningen et al. [1] and Grafsrønningen and Jensen [2]. Large scale heat exchangers based solely upon natural convection heat transfer may consist of multiple horizontal cylinders connected at the ends using pipe bends forming meandering tubes, cf. Gyles et al. [3] for an example. A transition will influence the transport and mixing properties downstream the cylinder significantly. Hence, a transition may influence the efficiency and design of heat exchangers greatly and it is therefore important that the transition is captured in the simulations. It is generally recognized that RANS-models are unable to predict laminar to turbulent transitions. However,

as pointed out by Durbin and Reif [4] RANS simulations tend to approach either the laminar or turbulent solution.

Kuehn and Goldstein [5] studied laminar natural convection heat transfer from a horizontal cylinder by solving the Navier-Stokes equations and the energy equation using a finite difference technique. Similarly to Kuehn and Goldstein [5], Farouk and Güçeri [6] investigated laminar natural convection heat transfer from isothermal and anisothermal horizontal cylinders using a finite difference technique. Farouk and Güçeri [7] then investigated turbulent natural convection heat transfer numerically for Rayleigh numbers ranging from 5E7 to 1E10. Several other researchers have investigated natural convection heat transfer from horizontal cylinders, see Grafsrønningen and Jensen [8] for a more detailed overview of some of the available literature.

It has been established that RANS-models are unable to predict transition from laminar to turbulent flow. Nevertheless, in engineering LES may not be feasible due to lack of computational resources, a proper LES-code, or for other reasons. Hence, RANS may be the only available simulation tool. Thus the authors have recognized the need for RANS simulations with commercial general purpose CFD-tools of a transitional buoyant plume above a heated horizontal cylinder with a thorough comparison against experimental results.

Simulations

Turbulent flows driven by thermal buoyancy is particularly demanding to RANS according to Hanjalić [9]. These flows feature strong pressure fluctuations, inherent unsteadiness and energy nonequilibrium which hardly are captured by RANS. As stated by Hanjalić [9]: "It is generally recognized that the two-equation $k-\varepsilon$ and similar eddy-viscosity models with linear stress-strain relations and their analogue for scalar fields cannot reproduce any flows with significant nonequilibrium effects, flows subjected to body forces or to any extra-strain rates other than simple shear." A deficiency to the linear eddy viscosity assumption follow from representing the turbulence solely by the turbulent kinetic energy k. External forces often act on one component more strongly than others, thus a single scalar k is largely unable to emulate such features, see Durbin and Reif [4]. Second-moment closures on the other hand, offers a more solid physical platform. Equations for Reynolds stresses are solved rather than approximated through an eddy-viscosity approach. However, modelling of a number of terms in the Reynolds stress equations is required to close the set of equations.

A number of second-moment models exists in the literature, yet probably the most popular is the $k-\varepsilon$ equivalent Reynolds-stress model. The model solves a set of equations for the Reynolds stresses $\overline{u_i u_j}$ in addition to an equation for the turbulence dissipation rate ε. However, Reynolds stress models with ε-equations are known to fail when applied to low Reynolds number flow such as boundary layer flow. An eddy-frequency ω-formulation is more suited to predict such flows, see ANSYS (p.100) [10]. Moreover, the ω-equation is known to fail in freestreams, such as in a buoyant plume, therefore models which combine the ω and ε effects have been developed. The Baseline Reynolds Stress Model (BSL RSM) is such an model, where the ω-formulation is used close to solid boundaries whereas the ε-equation is used in the freestream, see ANSYS (p.101) [10].

Boundary layers in high Reynolds number flow are very thin, hence wall-functions are of-

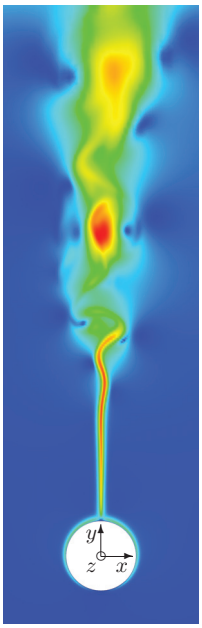

Figure 1: Instantaneous velocity field BSL RSM

ten used in commercial RANS-codes to account for wall effects without the need for very small computational cells close to the wall. Generally a y^+ of 200 or less is required in modern CFD-codes. However, most wall-functions are developed for high Reynolds number flow. Thus they do not work for natural convection. Barakos et al. [11] assessed the effect of wall-functions on heat transfer in a square cavity convection cell and concluded that the Nusselt number was significantly overpredicted. The Nusselt number was overestimated with 50%-100% depending on the Rayleigh number. Some RANS-models have automatic wall treatments, i.e. if sufficiently resolved ($y^+ \simeq 1$) wall-functions are not used, and a low Reynolds number formulation is used instead, see ANSYS (p.61) [12]. Hence, the ensemble averaged equations are solved for the entire domain without an approximation close to walls which is required to predict the wall heat transfer in natural convection correctly. The ω-formulation in the BSL RSM cope with low Reynolds number flows close to solid boundaries. Wall functions for turbulent natural convection flow are constantly being developed, but have generally not yet found their way into commercial CFD-codes, see e.g. Kǐs and Herwig [13].

Another problem with RANS for buoyant turbulent flows is the lack of uniform scaling. One-point closures generally use uniform turbulence length and time scales. According to Hanjalić [9] DNS and LES are required to capture the large scale structures. However, a middle way may be chosen as an attempt to use RANS-relations on flows which generally require LES or even DNS to solve. URANS is unsteady RANS where large scale features are resolved in time and space, see e.g. Hanjalić [9] or Hanjalić and Kenjereš [14]. No known one-point closure level is satisfactory for three-dimensional flows with dominating large-scale eddy structures. Though an unsteady RANS approach may, according to Hanjalić [9], capture coherent

p_1	-0.000000029508602
p_2	0.000011218941671
p_3	-0.001040500036804
p_4	0.031687468152510
p_5	21.20760727142974

Table 1: Coefficients for thermal boundary condition polynomial $T(\theta) = p_1\theta^4 + p_2\theta^3 + p_3\theta^2 + p_4\theta + p_5 + T_\infty$. $\theta = 0$ is at the lower stagnation point, T_∞ is 20.89°C.

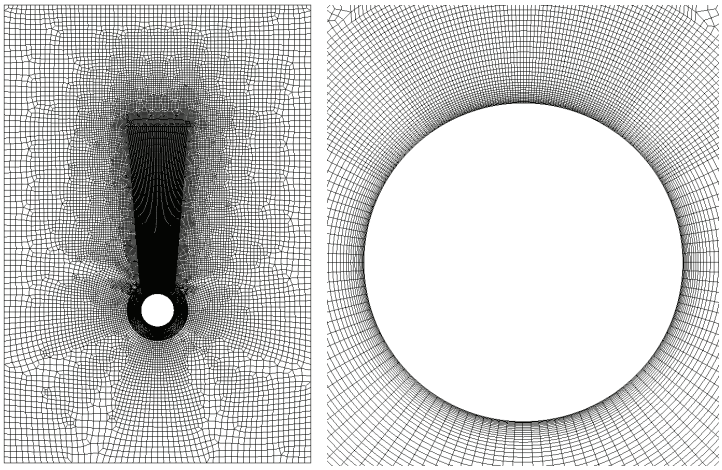

Figure 2: Computational mesh and close up view

structures and reproduce all flow and heat transfer parameters.

One may argue that URANS is LES in a RANS framework. LES models accounts for turbulent effects smaller than the computational grid, whereas RANS models accounts for turbulent effects on all wave numbers. As pointed out by Hanjalić [9], RANS models are unable to predict large scale features and an unsteady approach is required to emulate such flows. Thus the large scales are not modelled in an URANS approach, and the two methods are rather coincident. Though, contributions from LES models depend on the spatial resolution, whereas input from RANS models do not. For an increasingly finer spatial resolution, contributions from LES models vanish, and the simulation eventually becomes a DNS, given that the time step and numerics are treated accordingly. RANS model output does not change with spatial resolution, given that mesh convergence is achieved, hence the two approaches differ to some extent. Furthermore, LES require three-dimensional simulations, whereas, in general, two-dimensional RANS simulations may be carried out given that there is a periodic directionality.

Following Hanjalić [9] suggestions, unsteady RANS of the heated horizontal cylinder was attempted. Among others the Baseline Reynolds stress model implemented in CFX (v.12.0.1) was chosen for the RANS simulations, see ANSYS [15]. The Baseline Reynolds stress model should be able to handle the buoyant free-stream as well as low-Reynolds number flow close to the wall. The Baseline Reynolds stress model implementation in CFX allows for a fine mesh normal to solid walls without using wall models. Hence, a low-Reynolds formulation is used within the boundary layer. However, the model is most likely not able to predict the transition

onset. Nevertheless, as mentioned earlier, a proper LES-code may not be available in engineering. Thus RANS may be the only tool available. Hence, an assessment of the performance of RANS simulations of the transitional plume downstream an evenly heated horizontal cylinder is of interest.

Simulations using other turbulence models such as the Shear-Stress Transport (SST), Baseline Explicit Reynolds Stress Model (BSL EARSM), and the Speziale, Sarkar and Gatski Reynolds Stress Model (SSG RSM) were also carried out, see ANSYS [10]. Additionally, a simulation without any model was also carried out, i.e. a laminar simulation without any contributions from turbulence models. The BSL, SST and BSL EARSM use a $k-\omega$ formulation close to walls whereas in the freestream a $k-\varepsilon$ formulation is used, hence no wall models are used given that the wall normal grid resolution is adequate. The SSG RSM and $k-\varepsilon$ models use a wall-function to approximate the flow and thermal fields close to walls regardless of the near wall grid resolution.

Some modern commercial general purpose CFD-codes have implemented laminar-turbulent transition models which predicts the transition onset based on local variables. Generally the transition models solve transport equations for the intermittency factor γ and the transition momentum thickness Reynolds number $\overline{Re}_{\theta t}$, see Menter et al. [16]. However, these formulations are made for wall bounded flows and similar configurations and they generally does not work for other types of flow. However, the intermittency factor γ may be specified otherwise if empirical correlations or other information about the transition onset exist. The intermittency factor γ is included in the turbulent kinetic equation (for a two-equation closure model) where $0 < \gamma < 1$ controls the production and destruction of turbulent kinetic energy.

Simulations using specified intermittency γ as a transition criteria in conjunction with the Shear-Stress Transport model (SST) was carried out. The transition criteria was specified using the local Grashof number $Gr_{Q,Y} = \frac{g\beta Q y^3}{\rho C_p \nu^3}$, see e.g. Noto et al. [17]. The intermittency factor was $\gamma = H(Gr_{Q,y} - Gr_{Q,y,Tr})$ where H is the Heaviside function and $Gr_{Q,y,Tr} = 2E8$ is the transitional local Grashof number given by Noto et al. [17], i.e. where transition initiated. Hence, γ is either zero or unity, depending on the relative distance downstream the cylinder and dissipated power per length Q $[W/m]$. y_{tr} is the distance downstream cylinder center which corresponds to $Gr_{Q,y,Tr} = 2E8$.

The computational domain is two-dimensional, 10D wide and 15D tall, the cylinder is located 5D above the domain bottom. Open boundary conditions in conjunction with a relative pressure and low turbulence intensity were specified at the domain boundaries which allows for both in and outflow. A polynomial $T(\theta)$ fitted to the experimental data, was specified as the thermal boundary condition, see table 1. A maximum CFL-number of 1.0 was used in the simulation. The simulations were run for about 25000 timesteps after statistical steady state conditions were achieved, which is equivalent to about 4 min. Unsteady simulations were carried out with all models, although the two-equation models did not require such an approach, the SST and $k-\varepsilon$ models produced steady results. A three-dimensional simulation using the BSL RSM was carried out and compared to the results from the two-dimensional simulation. No discernible differences between the two and three-dimensional simulations were found, hence two-dimensional simulations were carried out for the other models.

The smallest eddies in a turbulent flow is characterized by the Kolmogorov length scale $\eta = (\nu^3/\varepsilon)^{1/4}$, cf. e.g. Pope [18]. However, in thermal flows with Prandtl number much larger

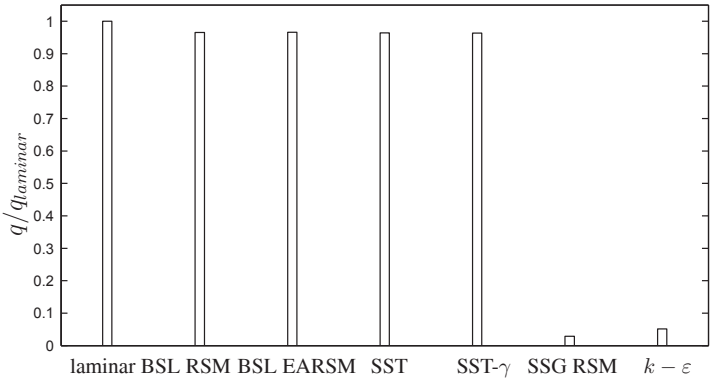

Figure 3: Average cylinder wall heat flux for different simulations.

than unity the smallest scales are described by another scale, namely the "conduction cut-off", see Batchelor [19]. He gave an expression for the conduction cut-off expressed in terms of kinematic viscosity ν, thermal diffusivity α and the dissipation rate ε, namely $\eta_B = (\nu\alpha^2/\varepsilon)^{1/4}$. The smallest viscous scale may be expressed as

$$\eta = Gr^{-(3/8)}D \tag{1}$$

where the turbulence dissipation rate is approximated as $\varepsilon = U_0^3/L = (g\beta\Delta T D)^{3/2}/D$. The conduction cut-off scale is

$$\eta_B = Gr^{-(3/8)}Pr^{-1/2}D. \tag{2}$$

Thus the wall normal grid spacing was specified to $y^+ = y/\eta_B = 0.89$ which is adequate to avoid use of wall-functions for the blended $\varepsilon - \omega$-based models.

Results

Figure 3 shows the average cylinder wall heat flux from each of the simulations. The flow around the cylinder is laminar, turbulent effects crop up downstream the cylinder, hence the laminar simulation should provide the correct results. Neglecting turbulent effects downstream the cylinder should not effect the computed heat flux nor the flow field around the cylinder in the laminar simulation. The average wall heat flux is within the experimental uncertainty, thus the laminar result is used as a reference for the other simulations. The blended $\varepsilon - \omega$-based simulations, i.e. the BSL RSM, BSL EARSM, SST and SST-γ models underpredicts the heat flux with about 3.5% compared to the laminar result.

The SST-γ simulation, where the production and destruction terms in the k-equation was suppressed in cylinder vicinity, yields the same results as the other blended $\varepsilon - \omega$-based simulations. Thus contributions from turbulent convection $\overline{u_i u_j}$ are small, hence the BSL RSM, SST and SST-γ simulations all approach the laminar results around the cylinder without any intermittency modeling. The SSG and $k - \varepsilon$ models, which use wall models, underpredicts the heat flux significantly. The ε-models underestimates the heat flux with factors of 35 and 20 for the SSG and the $k - \varepsilon$ models respectively. An accurate wall heat flux prediction is a prerequisite

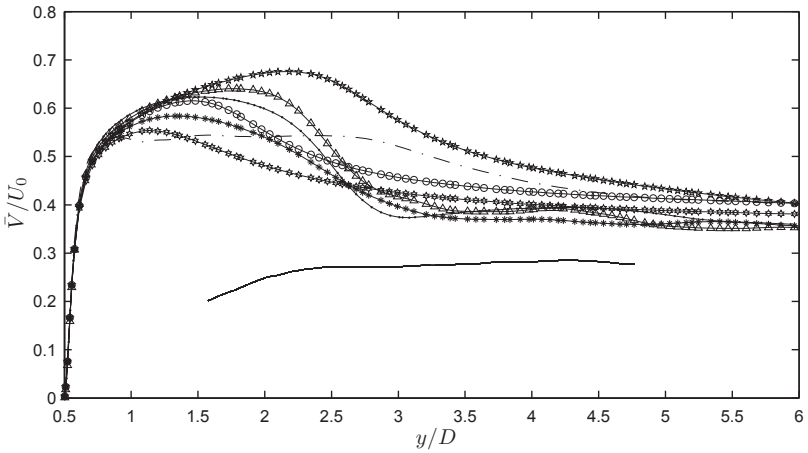

Figure 4: Vertical velocity in plume center normalized against the characteristic velocity $U_0 = \sqrt{g\beta\Delta TD}$. $*$ BSL RSM, $\triangle$ laminar, $\circ$ SST, $\star$ SST with intermittency, LES results (dash-dotted line – Grafsrønningen et al. [8]), and experimental results (solid line – Grafsrønningen and Jensen [2])

in buoyant flows from heated objects. Thus the velocity and temperature fields downstream the cylinder will be incorrect due to the qualitatively wrong heat flux predictions.

Figure 4 shows vertical velocity in plume center for the blended $\varepsilon - \omega$-based models, the laminar simulation, experimental results from Grafsrønningen and Jensen [2], and LES results from Grafsrønningen et al. [8]. Results from the SSG and $k - \varepsilon$ models are not included due to the wrongfully predicted heat flux. LES results are included for comparison with laminar and RANS results. The BSL RSM and laminar results are relatively similar, the results differ marginally upstream $2y/D$. Further downstream the BSL RSM results decelerates at a slower rate than the laminar results, though the results are still rather like. A comparison of the plume growth and widths show that the BSL RSM and laminar results are near identical (not shown here). The SST and the SST$-\gamma$ results, SST$-\gamma$ in particular, overpredicts the vertical velocity in plume center compared to the laminar and BSL RSM results. However, all results deviate significantly from the experimental results, even the LES results differ considerably.

Figure 5 shows the BSL RSM results $a)$ and experimental results $b)$. The same is observed here as in Figure 4 where the vertical velocity is highly overpredicted in the lower part of the plume, i.e. in close vicinity to the cylinder. Further downstream the plume center velocity approaches the experimental data, but is still significantly larger than the experimental data. The temperature excess ΔT is also higly overpredicted. However, the plume width, particularly far downstream, is similar to the experimental data.

An assessment of the contribution from the turbulent eddy viscosity ν_t, or its analogue for second-moment closures, show that there is a minuscule input from the models. Hence, all simulations approach the laminar solution in the entire domain. As mentioned in the previous section the turbulent boundary conditions were specified as "low intensity", i.e. the turbulent intensity was set to 1%. Simulations with other turbulent boundary conditions were carried out with no discernible differences. Even for relatively extreme turbulent boundary conditions the results approach the laminar solution.

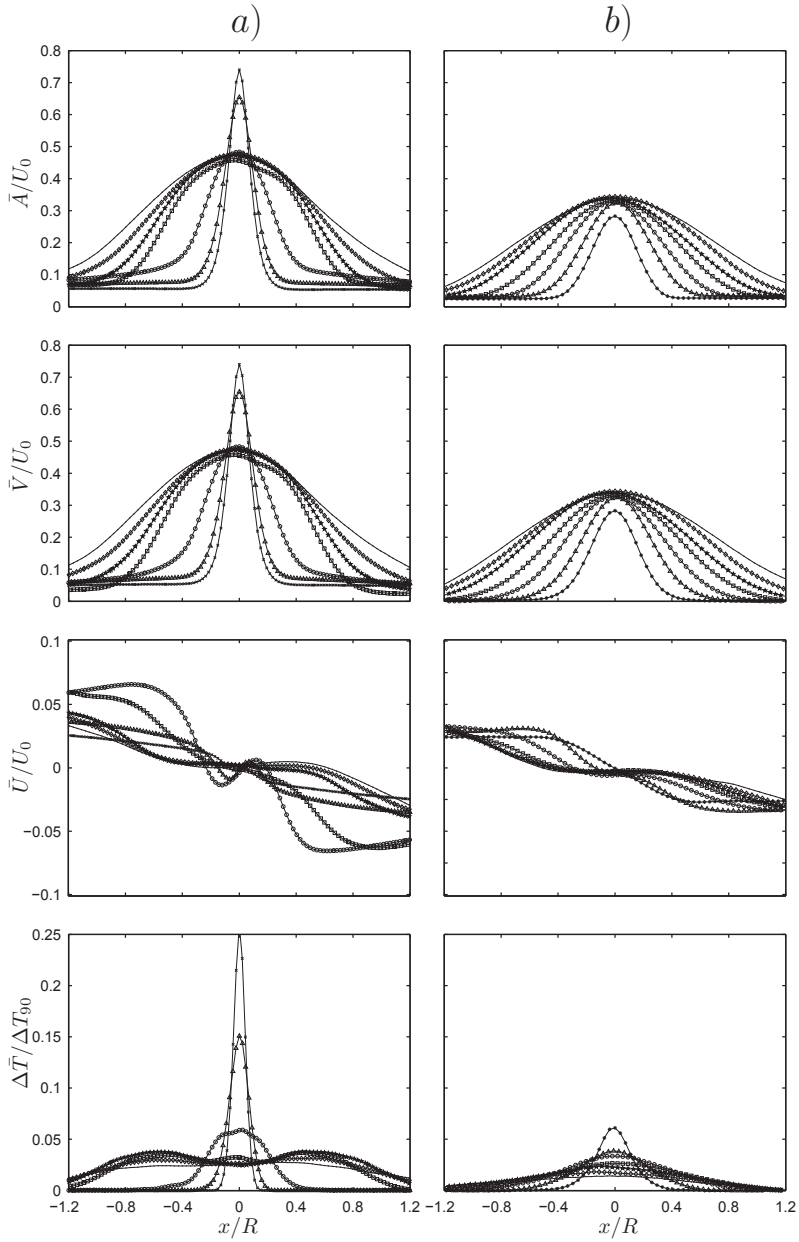

Figure 5: a) RANS b) experiments – Velocity magnitude A, vertical velocity V, horizontal velocity U, and temperature excess $(T - T_\infty) * 100mm$, $\triangle$ $125mm$, $\bigcirc$ $150mm$, $\square$ $175mm$, $\star$ $200mm$, $\diamond$ $225mm$, $\cdot$ $250mm$ above cylinder center.

Additional simulations with models based on the turbulent eddy frequency ω-formulation, such as the $k - \omega$ and ω-RSM, were also carried out. Though, the outcome was more or less the same, the results resembles the laminar solution.

Conclusion

Unsteady RANS simulations of a heated horizontal cylinder in water is carried out and compared with experimental data. Different one-point closure models were attempted, both two-equation turbulence models, and more sophisticated second-moment models were used. The second-moment models are generally superior to their linear eddy viscosity counterparts in buoyant turbulent flows and for flows with strong anisotropy, they offer a more physically sound platform compared to models using linear stress-strain relations. However, the second-moment models require extensive modeling. The results show that all simulations overpredict the vertical velocity and temperature excess in the plume downstream the cylinder compared to the experimental data significantly. A laminar simulation, i.e. without any turbulence models, and simulations using the BSL RSM, yielded the best results.

Results from simulations with ε-models which rely on wall-functions to predict wall shear and wall heat flux proved wrong. The wall-functions are developed for high Reynolds number forced convection and are generally unable to predict correct wall heat flux in natural convection. The wall-functions underestimate the wall heat transfer from the cylinder with factors of more than 20, depending on the model. Simulations with models which combine the best features of eddy frequency ω-formulations and turbulent kinetic energy dissipation ε-formulations gave the best results due to rather accurate wall heat flux predictions.

Natural convection heat transfer from horizontal cylinder at intermediate Rayleigh numbers involve a laminar to turbulent transition downstream the heated cylinder. Such features are generally not tractable by RANS models. Intermittency modeling may in some cases fascilitate RANS simulations of transitional flows. However, the results approach the laminar solution regardless of the model used. Hence, intermittency modeling will not aid prediction of the transitional buoyant flow over a heated horizontal cylinder.

Nevertheless, although CFD simulations of a single cylinder fail due to laminar to turbulent transitional effects, in engineering, natural convection from a single heated horizontal cylinder is hardly of interest. CFD is used in design of large scale, complex heat exchangers. Thus laminar-turbulent transitions may only occur in a limited area. Hence, fully turbulent simulations, where the models produce the turbulent solution rather than approaching the laminar solution, may serve as a reliable design tool. Intermittency models based on empirical correlations may be used to enforce a laminar solution upstream a point of transition. Furthermore, a heat exchanger based solely on natural convection heat transfer may consist in the order of 10×40 (width/height) staggered tubes, see e.g. Gyles et al. [3]. The induced buoyant flow will quickly develop to a turbulent flow in the far lower part of the heat exchanger. Hence, without any intermittency modeling, erroneous results may be limited to the lower row of cylinders, i.e. where a turbulent solution is produced by the CFD-tools and the flow is laminar. Further downstream the flow will be turbulent, thus the CFD-tools in conjunction with suitable turbulence models have all the prerequisites to produce the correct solution.

Acknowledgments

Financial support for this work was provided by the PETROMAKS project under research grant no. 193215/S60 from the Norwegian Research Council.

Bibliography

[1] S. Grafsrønningen, A. Jensen, and B.A.P. Reif. PIV investigation of buoyant plume from natural convection heat transfer above a horizontal heated cylinder. *International Journal of Heat and Mass Transfer*, 54:4975–4987, 2011.

[2] S. Grafsrønningen and A. Jensen. Simultaneous PIV/LIF measurements of a transitional buoyant plume above a horizontal cylinder. *International Journal of Heat and Mass Transfer*, 55:4195–4206, 2012.

[3] B.R. Gyles, B. Hægland, T.B. Dahl, A. Sanchis, S. Grafsrønningen, R.B. Schüller, and A. Jensen. Natural convection - subsea cooling; theory, simulations, experiments and design. *Proceedings of the ASME 30th International Conference on Ocean, Offshore and Arctic Engineering*, 2011.

[4] P.A. Durbin and B.A.P. Reif. *Statistical theory and modeling for turbulent flows*. John Wiley and Sons Inc., 2003.

[5] T.H. Kuehn and R.J. Goldstein. Numerical solution to the Navier-Stokes equations for laminar natural convection about a horizontal isothermal circular cylinder. *International Journal of Heat and Mass Transfer*, 23:971–979, 1980.

[6] B. Farouk and S.I. Güçeri. Natural convection from a horizontal cylinder - laminar regime. *Transactions of the ASME*, 103:522–527, 1981.

[7] B. Farouk and S.I. Güçeri. Natural convection from a horizontal cylinder - turbulent regime. *Transactions of the ASME*, 104:228–235, 1982.

[8] S. Grafsrønningen, A. Jensen, and B.A.P. Reif. Large eddy simulation of a buoyant plume above a heated horizontal cylinder at intermediate rayleigh numbers. *Submitted to International Journal of Heat and Mass Transfer*, 2012.

[9] K. Hanjalić. One-point closure models for buoyancy driven turbulent flows. *Annual Review of Fluid Mechanics*, 34:321–347, 2002.

[10] ANSYS Inc. *ANSYS CFX-Solver Modeling guide*, release 12.0 edition, April 2009.

[11] G. Barakos, E. Mitsoulis, and D. Assimacopolous. Natural convection flow in a square cavity revisited: laminar and turbulent models with wall functions. *International Journal for Numerical Methods in Fluids*, 18:695–719, 1994.

[12] ANSYS Inc. *ANSYS CFX Referance Guide*, release 12.0 edition, April 2009.

[13] P. Kiš and H. Herwig. The near wall physics and wall functions for turbulent natural convection. *International Journal of Heat and Mass Transfer*, 55:2625–2635, 2012.

[14] K. Hanjalić and S. Kenjereš. 'T-RANS' simulation of deterministic eddy structure in flows driven by thermal buoyancy and lorentz force. *Flow, Turbulence and Combustion*, 66:427–451, 2001.

[15] ANSYS Inc. *ANSYS CFX-Solver Theory guide*, release 12.0 edition, April 2009.

[16] F.R. Menter, R. Langtry, and S. Völker. Transition modelling for general purpose CFD codes. *Flow Turbulence Combust*, 77:277–303, 2006.

[17] K. Noto, K. Teramoto, and T. Nakajima. Spectra and critical Grashof numbers for turbulent transition in a thermal plume. *Journal of Thermophysics and Heat Transfer*, 13:82–90, 1999.

[18] S.B. Pope. *Turbulent flows*. Camebridge University Press, 2000.

[19] G.K. Batchelor. Small-scale variation of convected quantities like temperature in turbulent fluid. Part 1. general discussion and the case of small conductivity. *Journal of Fluid Mechanics*, 5(1):113–133, 1959.

Miscellaneous

In the course of this project I have attended two academic conferences, namely *The 6th Symposium on Turbulence, Heat and Mass Transfer* in Rome, Italy in 2009, and the *EUROMECH conference ETC13 – 13th European Turbulence Conference* in Warsaw, Poland in September 2011, where I gave a presentation entitled ”PIV investigation of a buoyant plume above a heated horizontal cylinder“. The presentation at *ETC13* was based on work carried out in colloboration with my supervisors Professor Jensen and Professor II Reif.

Further, I had a five week stay at Cornell University, Ithaca, USA, in the beginning of 2012, where I worked together with Professor Jensen during his sabbatical stay there.

In addition to the activities described throughout this thesis, Professor Jensen and I have applied for a patent together with the University of Oslo and Inven2. Inven2 is a UIO-owned innovation company working to commersialize ideas emerging from the University of Oslo. The patent is based on an idea which emerged from one of our experimental investigations. A patent application was filed in April 2011 and a decision is expected in medio October 2012. Professor Jensen and I won the Inven2 award for 2011 for our idea.